PRAMANA
— journal of
physics

Vol. 44, No. 2,
February 1995
pp. 183–200

Trinucleon system with Reid soft core potential by hyperspherical harmonics expansion method

SATADAL BHATTACHARYYA and TAPAN KUMAR DAS*
Department of Physics, Burdwan University, Burdwan 713 104, India
*Department of Physics, Calcutta University, 92 APC Road, Calcutta 700 009, India

MS received 6 June 1994; revised 15 October 1994

Abstract. The hyperspherical harmonics expansion method has been used to solve the trinucleon system where the nucleons interact through Reid soft core potential. The binding energy of triton, both for extreme adiabatic approximation and uncoupled adiabatic approximation, and the S-state, S'-state and D-state probabilities are calculated and compared with the results by the Faddeev method.

Keywords. Nuclear structure; few body system; hyperspherical harmonics expansion method; Reid soft core potential.

PACS Nos 21·40; 21·10

1. Introduction

Since the development of the hyperspherical harmonics expansion (HHE) method [1–5] in the early seventies, it has been applied profitably for the determination of the bound state properties of a few nucleon systems [1–6] as well as light atomic and molecular systems [8]. In this method, the wave-function is expanded in an infinite series of generalized partial waves and the Schrödinger equation gives rise to an infinite set of coupled differential equations (CDE). Although the size of the expansion basis can be reduced by the introduction of the optimal subset [5], the sum over the hyperangular momentum quantum number (K) must be truncated in order to get a finite set of CDE, to be numerically tractable. Convergence of the expansion is slow, unless the potential is very soft. The usual criterion for the truncation of the expansion basis with respect to K is the attainment of convergence in binding energy (BE) up to a predetermined limit. This however does not guarantee an attainment of convergence in the asymptotic part of the wave-function and thus the wave-function (particularly the asymptotic part of it) is less reliable than the BE.

The HHE method is also not easily adoptable when the interaction potential is dependent on the state of the interacting particles, as in realistic nucleon nucleon (NN) potentials. This is the reason why the HHE method has so far been applied to nuclear problems with simple S-projected, relatively soft potentials only. Moreover such potentials are usually chosen to be a sum of Gaussians or exponentials, which although are convenient for a fast convergence, but still do not have the necessary one pion exchange tail. Hence the asymptotic part of the wave-function as determined by the asymptotic normalization constants, is not reliable [7] and cannot be compared with calculations by other methods or with experimental numbers. Nevertheless the

HHE method is interesting since it deals directly with the wave-functions and hence provides a clear physical picture.

The other and perhaps the most frequently used essentially exact technique to solve the three body problem is the Faddeev equation method [9]. In this approach, for a given partition of the three body system, the angular momentum quantum numbers of the interacting pair and those of the spectator particle specify the characteristics of each channel, for which Faddeev equations are written separately. This approach is particularly suited to realistic NN potentials. On the other hand inclusion of a long range interaction like the Coulomb potential, involving a large number of partial waves, is inconvenient in traditional momentum space Faddeev calculations. However, this problem does not arise in coordinate space Faddeev calculation, for which sophisticated numerical techniques have been developed [12]. One of the most commonly employed realistic NN potentials is the Reid soft core [10] (RSC) potential, which depends on the spin (s), isospin (t) and total angular momentum (j) of the interacting pair and thus the Faddeev equation method is suitable to deal with such an interaction. On the other hand, the calculation of matrix elements of this potential necessary for the HHE method becomes extremely complicated. For this reason, while there is an abundance of Faddeev calculation with the RSC potential [11–13], no attempt has so far been made to find the complete solution of the trinucleon system by the HHE method with this potential, although several works have been reported with simple potentials [1–6].

As has already been mentioned, the reliability of the asymptotic wave-function obtained by the HHE method has not been established. On the other hand, the asymptotic wave-function strongly depends on the correctness of the asymptotic part of the NN interaction chosen. To throw light on the convergence and correct behaviour of the asymptotic wave-function obtained by HHE method, it is necessary to solve the trinucleon system by this method with a realistic potential, having appropriate asymptotic behaviour. We have chosen the RSC potential for this purpose, for which Faddeev results are available for comparison. As a first step towards this goal, we have calculated in the present work the binding energy of triton using RSC potential by the HHE method. Mukhtarova [14] performed accurate HHE calculations with some of the realistic NN potentials like GPT [15], SSC [16], TRS [17] potentials etc, but RSC was not used by her. To the best of our knowledge, this is the first calculation of the trinucleon system by the HHE method using RSC potential. Adiabatic approximation has been used to approximately decouple the resulting equations. Convergence behaviour of the binding energy in the extreme and uncoupled adiabatic approximation (EAA and UAA respectively) have been studied. For the best computer facility available, we have been able to retain up to a maximum K value of 15 for each symmetry component, which gives the EAA and UAA binding energy to within about 1·3%. Following a theorem on the convergence of hyperspherical harmonics expansion by Schneider [18], a semiempirical extrapolation formula has been obtained for the missing binding energy. These results together with the probabilities of S, S' and D states have been compared with the earlier calculation by Faddeev method.

This paper is organized as follows. Section 2 contains a brief review of the HHE theory and its adoption to the RSC potential. In § 3, we present the results obtained and discuss the convergence behaviour. Conclusions have been drawn in § 4. Appendix A is provided for the coupling matrix elements. For clarity of our discussion the various components of the RSC potential are presented in Appendix B.

2. The theory

This section is divided into two subsections: in the first the coupled differential equations (CDE) are set up for realistic potentials and in the second the coupling matrices for the RSC potential are developed.

A. Coupled differential equations

The relative motion of trinucleon system is described in terms of the Jacobi coordinates

$$\mathbf{x} = \mathbf{r}_2 - \mathbf{r}_1$$
$$\mathbf{y} = 2/\sqrt{3}[\mathbf{r}_3 - (\mathbf{r}_1 + \mathbf{r}_2)/2], \tag{1}$$

where $\mathbf{r}_i$ is the position of the ith nucleon. The hyperradius r, defined through

$$r^2 = x^2 + y^2, \tag{2}$$

is invariant under exchange of any pair of nucleons and three dimensional rotations. The hyperangular set $\{\Omega\}$ describing the five other space degrees of freedom is constituted by four spherical polar angles $\hat{x}(\theta_x, \phi_x)$ and $\hat{y}(\theta_y, \phi_y)$ giving the orientations of $\mathbf{x}$ and $\mathbf{y}$ and one hyperspherical angle ϕ defined in terms of relative lengths of x and y by

$$\tan\phi = y/x, \quad 0 \leqslant \phi \leqslant \pi/2. \tag{3}$$

The wave-function is expanded in a complete orthonormal set of hyperspherical harmonics [5] as

$$\psi_{JM_J}^{TM_T}(r, \Omega) = \sum_{K,\varepsilon,T,S} n(\varepsilon) r^{-5/2} U_{2K+L}^{\varepsilon,T,S}(r)[{}^{\varepsilon}B_{2K+L}(\Omega) \otimes \Gamma_{TS}(\varepsilon^*)]_J^{M_J} \tag{4}$$

where T, S and L correspond to total isospin, spin and orbital angular momentum respectively and $\mathbf{J} = \mathbf{L} + \mathbf{S}$ is the total angular momentum; ε specifies the symmetry of the spatial part of the wave-function under exchange of particles, which can be the totally-symmetric S, mixed symmetry S'^+, S'^- and D^+, D^- states; the + or − signs correspond to symmetry or antisymmetry under the exchange of (12) pair of particles. The spectroscopic notations S and D correspond to $L = 0$ and $L = 2$ respectively, L being the total angular momentum. The factor $n(\varepsilon)$ is defined as

$$n(\varepsilon) = 1 \text{ for } S \text{ state}$$
$$= 1/\sqrt{2} \text{ for } S'^+, D^+ \text{ and } D^- \text{ states}$$
$$= -1/\sqrt{2} \text{ for } S'^- \text{ state.}$$

$\Gamma_{TS}(\varepsilon^*)$ is the isospin-spin state of three nucleon system with total isospin T and total spin S and having a symmetry conjugate to ε, such that $[{}^{\varepsilon}B_{2K+L}(\Omega) \otimes \Gamma_{TS}(\varepsilon^*)]_J^{M_J}$ is totally antisymmetric. It is given by

$$\Gamma_{TS}(\varepsilon^*) = \sum_{s,t} b_s^t(\varepsilon^*) |(s\ 1/2) S M_S\rangle |(t\ 1/2)\ T M_T\rangle, \tag{5}$$

where s and t represent spin and isospin of the interacting pair and $b_s^t(\varepsilon^*)$ are coefficients determined by the symmetry requirement. An element of the appropriate optimal subset of hyperspherical harmonics is ${}^{\varepsilon}B_{2K+L}(r)$ (its explicit form is given in ref. [5]) and $[{}^{\varepsilon}B_{2K+L}\otimes\Gamma_{TS}(\varepsilon^*)]_J^{M_J}$ represents coupling of **L** and **S** to a total angular momentum J with z-component M_J (for the trinucleon $J=1/2$). The RSC potential depends on the angular momentum (j_1), spin(s) and isospin (t) of the interacting pair and the j_1 value ($\mathbf{j}_1=\mathbf{l}_1+\mathbf{s}$) is restricted to $j_1\leqslant 2$ (Appendix B). Thus it is convenient to express the spin-isospin hyperangular part of the wave-function, in $(j-j)$ coupling scheme:

$$
\begin{aligned}
&[{}^{\varepsilon}B_{2K+L}\otimes\Gamma_{TS}(\varepsilon^*)]_J^{M_J}\\
&\quad={}^{\varepsilon}N_{2K+L}\sum_{\substack{s,t\\ [l_1],[l_2]}} b_s^t(\varepsilon^*)|(t\,1/2)\,TM_T\rangle[(2l_1+1)(2l_2+1)/(2L+1)]^{1/2}\\
&\qquad\langle l_1 l_2 0\,0|\,L0\rangle\,{}^{\varepsilon}F_{2K+L}^{l_2,l_1}(\varphi)\\
&\qquad{}^{(2)}P_{2K+L}^{l_2,l_1}(\phi)\sum_{[j_1][j_2]}\begin{bmatrix} l_1 & l_2 & L\\ s & 1/2 & S\\ j_1 & j_2 & J\end{bmatrix}|(l_1 s)j_1,(l_2\,1/2)j_2;JM_J\rangle
\end{aligned}
\tag{6}
$$

where $[j_1],[l_1]$, etc represent restricted values as required from RSC potential. The normalization constant ${}^{\varepsilon}N_{2K+L}$ is given by

$$
{}^{\varepsilon}N_{2K}^{-2}=\sum_{[l_1]}(2l_1+1)|{}^{\varepsilon}F_{2K+L}^{l_1,l_1}(\varphi)|^2\times 0{\cdot}5\times\left[1+\sum_{[j_1][j_2]}\begin{bmatrix} l_1 & l_2 & 0\\ 1 & 1/2 & 1/2\\ j_1 & j_2 & 1/2\end{bmatrix}^2\right],
\tag{7}
$$

for the S and S' states and

$$
\begin{aligned}
{}^{\varepsilon}N_{2K+2}^{-2}=&\sum_{[l_1][l_2]}(2l_1+1)(2l_2+1)\begin{pmatrix} 2 & l_1 & l_2\\ 0 & 0 & 0\end{pmatrix}^2|{}^{\varepsilon}F_{2K+L}^{l_2,l_1}(\varphi)|^2\\
&\times\sum_{[j_1][j_2]}\begin{bmatrix} l_1 & l_2 & 2\\ 1 & 1/2 & 3/2\\ j_1 & j_2 & 1/2\end{bmatrix}^2
\end{aligned}
\tag{8}
$$

for the D state. The quantity ${}^{\varepsilon}F_{2K+L}^{l_2,l_1}(\varphi)$ is given by

$$
{}^{\varepsilon}F_{2K+L}^{l_2,l_1}(\varphi)=\sum_{\varepsilon}{}^{(2)}P_{2K+L}^{l_2,l_1}(\phi)
\tag{9}
$$

where ${}^{(2)}P_{2K+L}^{l_2,l_1}(\phi)$ is a hyperspherical function and Σ_ε acts on a function $f(\varphi)$ as:

$$
\sum_0 f(\varphi)=1/3[f(0)+f(2\pi/3)+f(-2\pi/3)],
\tag{10a}
$$

$$
\sum_+ f(\varphi)=1/3[2f(0)-f(2\pi/3)-f(-2\pi/3)],
\tag{10b}
$$

$$
\sum_- f(\varphi)=1/\sqrt{3}[f(-2\pi/3)-f(2\pi/3)].
\tag{10c}
$$

Substitution of (4) in the Schrödinger equation and projection on a particular hyperspherical harmonics leads to a system of coupled differential equations

$$\left[-\frac{h^2}{m}\left[\frac{\mathrm{d}^2}{\mathrm{d}r^2}-\frac{(2K+L+2)^2-1/4}{r^2}\right]-E\right]u^{\varepsilon TS}_{2K+L}(r)$$

$$+\sum_{K'\varepsilon'T'S'L'} C^{K\varepsilon TSL}_{K'\varepsilon'T'S'L'}(r)u^{\varepsilon'T'S'}_{2K'+L'}(r)=0, \tag{11}$$

where m is the nucleon mass, K represents the hyperangular momentum quantum number and $C^{K\varepsilon TSL}_{K'\varepsilon'T'S'L'}(r)$ is the coupling matrix elements explained in the next subsection.

B. *Coupling of the interaction*

The coupling matrix in (10) is given by

$$C^{K\varepsilon TSL}_{K'\varepsilon'T'S'L'}(r)=\pounds[{}^{\varepsilon}B_{2K+L}\otimes\Gamma_{TS}(\varepsilon^*)]^{MJ}_{J}\left|\sum_{i>j}V(r_{ij})\right|[{}^{\varepsilon'}B_{2K'+L}\otimes\Gamma_{T'S'}(\varepsilon'^*)]^{MJ}_{J}\circ \tag{12}$$

where $V(r_{ij})$ is the interaction potential of the (ij) pair. Detailed expressions for the coupling matrices for all possible combinations of RSC potential are already calculated [19]. The coupling between two states through central, $\mathbf{L}\cdot\mathbf{S}$ or tensor part can be obtained by using

$$\begin{aligned}&\langle(l_1s)j_1,(l_2\,1/2)j_2;JM_J|\,V_c+V_{LS}\mathbf{L}\cdot\mathbf{S}+V_TS_{12}|(l_1's')j_1',(l_2'\,1/2)j_2';JM_J\rangle\\&=\delta_{l_2l_2'}\delta_{j_2j_2'}[\delta_{l_1l_1'}\delta_{j_1j_1'}\delta_{ss'}\{V_C(r_{ij})+1/2\{j_1(j_1+1)-l_1(l_1+1)-s(s+1)\}^{1/2}\\&\times V_{LS}(r_{ij})\}+\delta_{ss'}\delta_{j_1,j_1'}\langle(l_1s)j_1|S_{12}|(l_1's)j_1\rangle V_T(r_{ij})]\end{aligned} \tag{13}$$

where $V_C(r_{ij})$, $V_{LS}(r_{ij})$ and $V_T(r_{ij})$ represent the radial dependences of central, $\mathbf{L}\cdot\mathbf{S}$ and tensor components of RSC potential (Appendix B). The matrix elements of the tensor operator S_{12} can be found in standard texts [20].

The possible component of RSC giving rise to coupling between (SS), $(S'S)$, $(S'S')$, (DS), (DS') and (DD) are given in table 1. Complete expressions for matrix elements of these blocks are given in Appendix A.

A typical term in the matrix element (12) contains (see Appendix A) an integral of the interaction potential and two ${}^{(2)}P^{l_2,l_1}_{L}$ functions [5], $\langle{}^{(2)}P^{l_2,l_1}_{2K+L}|\,V(r\cos\phi)|{}^{(2)}P^{l_2',l_2'}_{2K'+L}\rangle$, (note that $r_{12}=x=r\cos\phi$). Expressing the ${}^{(2)}P^{l_2,l_1}_{L}$ function in terms of Jacobi polynomials, this can be seen to be proportional to

$$I_{nn'}(r)=\int_{-1}^{1}P^{(\alpha,\beta)}_{n}(x)\,V(r_{12})P^{(\alpha',\beta')}_{n'}(x)(1-x)^{\gamma}(1+x)^{\delta}\mathrm{d}x \tag{14}$$

where $P^{(\alpha,\beta)}_{n}$ is a Jacobi polynomial and $\alpha=l_1+1/2$, $\beta=l_2+1/2$, $\gamma=(\alpha+\alpha')/2$, $\delta=(\beta+\beta')/2$; n,n' are determined from $2K+L=2n+l_1+l_2$ and $r_{12}=r((1+x)/2)^{1/2}$.

Since each of the element of the potential matrix contains contributions from several terms of the RSC potential (table 1 and Appendix A), a larger number of integrals of the type (14) are to be evaluated for each hyperradial mesh point. This would require an enormous computer time. The situation becomes more critical due

Table 1. Classification of different couplings.

Couplings	Components of RSC potential involved
SS	$V_C(^1S_0)$, $V_{C,LS}(^3S_1 - {}^3D_1)$, $V_C(^3D_2)$, $V_C(^1D_2)$
$S'S$	$V_C(^1S_0)$, $V_{C,LS}(^3S_1 - {}^3D_1)$, $V_C(^3D_2)$, $V_C(^1D_2)$
$S'S'$	$V_C(^1S_0)$, $V_{C,LS}(^3S_1 - {}^3D_1)$, $V_C(^3D_2)$, $V_C(^1D_2)$, $V_C(^1P_1)$, $V_C(^3P_0)$, $V_C(^3P_1)$, $V_{C,LS}(^3P_2 - {}^3F_2)$
DS	$V_T(^3S_1 - {}^3D_1)$
DS'	$V_T(^3S_1 - {}^3D_1)$, $V_T(^3P_2 - {}^3F_2)$
DD	$V_{C,LS,T}(^3S_1 - {}^3D_1)$, $V_C(^3D_2)$, $V_C(^3P_0)$, $V_C(^3P_1)$, $V_{C,LS,T}(^3P_2 - {}^3F_2)$

V_C, V_{LS} and V_T correspond to the central, LS and tensor component of the RSC potential.

to a large number of zeros of the integrand in the interval $[-1, 1]$ for large K, K' and so the numerical evaluation of the integral becomes tricky, requiring too large computer time for a specified precision. Instead, we evaluate the integral in (14) by expanding $V\{r[(1+x)/2]^{1/2}\}$ (whose typical form is as in (15)) in the complete set $\{P_{n''}^{(1/2,\,1/2)}(x)\}$

$$V(r(1+x)/2)^{1/2} = V_0 \frac{\exp\{-\mu r[(1+x)/2]^{1/2}\}}{(1+x)^{\rho/2}} = \sum_{n''=0}^{\infty} a_{n''}(r) P_{n''}^{(1,2,\,1/2)}(x) \tag{15}$$

where the potential multipoles $a_{n''}$ is given by

$$a_{n''}(r) = (1/h_{n''}^{1/2,\,1/2}) \int_{-1}^{1} V(r((1+x)/2)^{1/2}) P_{n''}^{(1/2,\,1/2)}(x)(1-x^2)^{1/2}\,dx, \tag{16}$$

$h_{n''}^{1/2,\,1/2}$ being the norm of Jacobi polynomial $P_{n''}^{(1/2,\,1/2)}$. Substitution of (15) in (14) gives

$$I_{nn'}(r) = \sum_{n''=0}^{\infty} a_{n''}(r) \langle n | n'' | n' \rangle \tag{17}$$

where the geometrical structure coefficients (GSC)

$$\langle n | n'' | n' \rangle = \int_{-1}^{1} P_n^{(\alpha,\beta)}(x) P_{n''}^{(1/2,\,1/2)}(x) P_{n'}^{(\alpha',\beta')}(x)(1-x)^{\gamma}(1+x)^{\delta}\,dx \tag{18}$$

is independent of the interaction potential as well as the hyperradius r. However eq. (17) is not advantageous unless the sum over n'' can be restricted. Since $P_n^{(\alpha,\beta)}$ is a polynomial of degree n in x, one can see from (18), by isolating one Jacobi polynomial together with its appropriate weight function and expressing the remain-

ing part of the integrand as a polynomial and using the orthogonality property of Jacobi polynomials that $\langle n|n''|n'\rangle = 0$ unless n'' satisfies $n_{\min} \leqslant n'' \leqslant n_{\max}$. Then (17) can be rewritten as

$$I_{nn'}(r) = \sum_{n''=n_{\min}}^{n_{\max}} a_{n''}(r)\langle n|n''|n'\rangle. \tag{19}$$

The GSC can itself be evaluated [21] by using the completeness property of Jacobi polynomials and solving a set of linear inhomogeneous equations (LIE). Note that the GSC need to be calculated once only and stored, to be used for each mesh point, resulting in an efficient and fast numerical procedure.

The above procedure will always work, except for the case when after isolating one Jacobi polynomial together with its weight function in the integrand of (18), the remaining part is not a polynomial. Such a situation can occur only for the tensor part of $({}^3S_1 - {}^3D_1)$ and $({}^3P_2 - {}^3F_2)$ interaction components. In this case one can include a factor of $(1-x)^{-1/2}$ with the potential function $V(r((1+x)/2)^{1/2})$, so as to make (19) valid once again. Although this extra factor introduces a singularity in $a_{n''}(r)$ (see (15) and (16)), it has been shown by us [22], that the principal value of this modified potential multipole exists for the cases under consideration and a numerical calculation produces sufficiently accurate results.

3. Results and discussion

The ground state of the trinucleon has dominant contributions from the totally symmetric $L=0$ state (S), mixed symmetry $L=0$ (S') and mixed symmetry $L=2$ (D) states only. The only other possibility, a P-state, has negligible probability and has been disregarded. With a maximum $K(=K_{\max})$ values of 15 for each of S, S', and D states, one has to solve a system of 46 coupled differential equations (CDE). Numerical algorithm for solving such a large number of CDE (for example, by renormalized Numerov method [23]) is very slow and not sufficiently stable. For this reason we have adopted the adiabatic approximation scheme [24] to solve the system of CDE. Due to the strong short range repulsion of the RSC potential, the convergence in binding energy (BE) with respect to inclusion of higher partial waves, is not expected to be sufficiently fast.

We have taken 300 uniform mesh points (of interval size 0·05 fm) for the hyperradial variable (r). For each mesh point the coupling potential matrix is calculated. As explained in the previous section, an appropriate multipolar expansion of each component of the RSC potential is made and the corresponding geometrical structure coefficients (GSC) are calculated by the LIE method [21] and stored (outside the r-loop). Then for each r-mesh point, all the potential multipoles are calculated and using the stored GSC, the potential matrix is computed. The diagonal hypercentrifugal part is added to this and then the matrix is diagonalized to obtain the lowest eigen potential ($w_0(r)$). All calculations have been done in double precision on an EISA 486 personal computer. In table 2a we demonstrate the convergence behaviour of $w_0(r)$ for a few selected values of r and for various values of K. It can be seen from this table, that the convergence of $w_0(r)$ is fairly rapid for small values of r, while it is quite slow for large values of r. Since a major part of BE comes from near the minimum of $w_0(r)$, convergence in BE is faster than the asymptotic wave-function. This is clearly seen in table 2b where calculated BE for various r_∞ (upper cut off in r) and for a few selected

Table 2a. Convergence of minimum eigenvalue ($-w_0(r)$) for various values of r.

	r(in fermi)						
K	1·8	2·15	2·55	3·05	4·05	7·55	10·05
8	23·344	35·639	30·550	22·494	12·695	0·479	—
9	23·459	35·880	30·865	22·739	13·091	1·201	−0·444
10	23·505	36·028	31·118	22·957	13·138	1·913	−0·189
11	23·525	36·087	31·258	23·189	13·247	2·739	0·162
12	23·535	36·109	31·335	23·331	13·384	3·456	0·560
13	23·536	36·116	31·368	23·425	13·497	4·018	1·000
14	23·538	36·119	31·383	23·479	13·624	4·532	1·544
15	23·539	36·122	31·390	23·505	13·718	4·617	2·095

Table 2b. BE in MeV in extreme adiabatic approximation for a few K with various r_∞.

	r (in fm)			
K	9·0	11·0	12·0	13·0
7	5·5478	5·5409	5·5401	5·5401
11	7·4581	7·4616	7·4612	7·4610
13	7·7812	7·7959	7·7963	7·7961
15	8·0113	8·0174	8·0178	8·0180

K values have been presented. A choice of 15 fm for r_∞ appears to be sufficient for reliability up to third decimal place. Figure 1 shows the behaviour of $w_0(r)$ as a function of r for $K_{max} = 15$. Using this $w_0(r)$ and the corresponding eigenvectors, approximately decoupled differential equations are obtained by the extreme and uncoupled adiabatic approximations [24] (EAA and UAA respectively). The decoupled equations have been solved by the Runge–Kutta method. Calculated BE by EAA ($-E_{EAA}$) and UAA ($-E_{UAA}$) together with incremental changes, have been presented in table 3. Convergence to 1·3% in both E_{EAA} and E_{UAA} have been achieved with $K_{max} = 15$ for each of S, S' and D states.

Calculated probabilities of S, S' and D states (P_S, $P_{S'}$ and P_D respectively) for various K values are shown in table 4. From this it is seen that P_D increases gradually (mostly at the cost of P_S) as K increases, indicating that the tensor coupling terms, having strong r dependence in short separation region, contribute significantly to higher partial waves, thereby enriching the D state. In figures 2 and 3 calculated hyperradial partial waves are plotted for various K values for S and D states. Since the computer time and memory requirements increase rapidy with increase of K_{max} values, we restricted our calculations to $K_{max} \leqslant 15$. However using the convergence theorems proved by Schneider [18], it is possible to estimate the converged energy by calculating the missing energy from a knowledge of the observed convergence trend for various K values. It was shown by Schneider that when the two-body potential is a sum of Yukawa terms, the convergence must be at least as fast as λ^{-4},

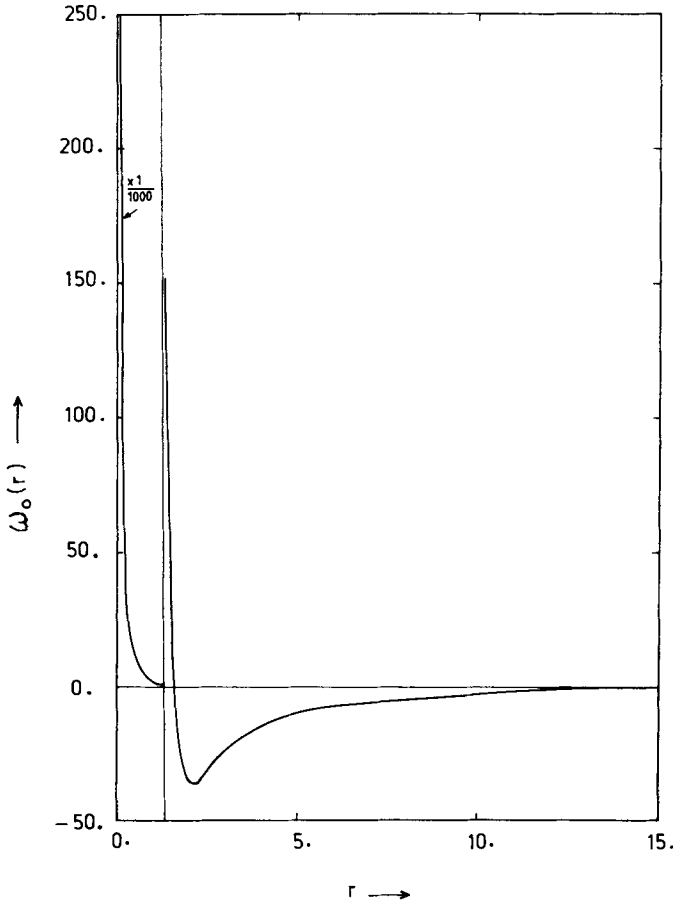

Figure 1. Lowest eigen potential, $\omega_0(r)$ as a function of r for $K_{max} = 15$.

where $\lambda = (K(K+4))^{1/2}$. Following Ballot *et al* [25] we define $\Delta E_K = |E(K+3) - E(K)|$ and assume

$$\Delta E_K = C(K+x)^{-4}, \tag{20}$$

where C and x are constants to be determined empirically. In table 5a, ΔE_K has been presented for $K = 3n$ (n is integer), which shows that the value of C in (20) is approximately constant. We least square fitted all calculated ΔE_K to the relation (20) to obtain C (24·272 and 24·266 for EAA and UAA respectively) and x (4·241 and 4·461 for EAA and UAA respectively). Using this, the estimated values of E_{EAA} and E_{UAA} for $K > 15$ are presented in table 5b, which shows the convergence is well established. Finally using (20) for $K \geqslant K_M$, where K_M is sufficiently large, we can estimate the converged energy as

$$E_\infty = E(K_M) + \sum_{n=0}^{\infty} \Delta E(K_M + 3n). \tag{21}$$

Table 3. BE of triton in MeV with extreme adiabatic approximation ($-E_{EAA}$) and uncoupled adiabatic approximation ($-E_{UAA}$).

K	$-E_{EAA}$	$-\Delta E_{EAA}$	$-E_{UAA}$	$-\Delta E_{UAA}$
5	2·928		2·204	
		1·742		1·582
6	4·670		3·786	
		0·870		0·781
7	5·540		4·567	
		0·830		0·771
8	6·370		5·338	
		0·515		0·476
9	6·885		5·814	
		0·292		0·276
10	7·177		6·090	
		0·283		0·269
11	7·460		6·359	
		0·207		0·192
12	7·667		6·551	
		0·129		0·123
13	7·796		6·674	
		0·124		0·119
14	7·920		6·793	
		0·098		0·089
15	8·018		6·882	

Table 4. Values of P_S, $P_{S'}$ and P_D.

K	$P_S\%$	$P_{S'}\%$	$P_D\%$
5	91·44	0·73	7·83
6	90·32	1·01	8·67
7	89·80	1·13	9·07
8	89·20	1·16	9·64
9	88·70	1·21	10·09
10	88·30	1·26	10·44
11	88·00	1·24	10·76
12	87·69	1·25	11·06
13	87·65	1·21	11·14
14	87·69	1·18	11·13
15	87·67	1·16	11·17

For sufficiently large K_M, one can replace the sum by an integral to get

$$E_\infty = E(K_M) + C\int_0^\infty \frac{dn}{(K_M + x + 3n)^4},$$

$$= E(K_M) + C\frac{1}{9(K_M + x)^3}. \tag{22}$$

Using (20) to evaluate $E(K_M)$ for $K_M = 45$ and then using (22) we obtain the convergent energies $-E_{EAA} = 8{\cdot}492$ MeV and $-E_{UAA} = 7{\cdot}339$ MeV. There are the upper and

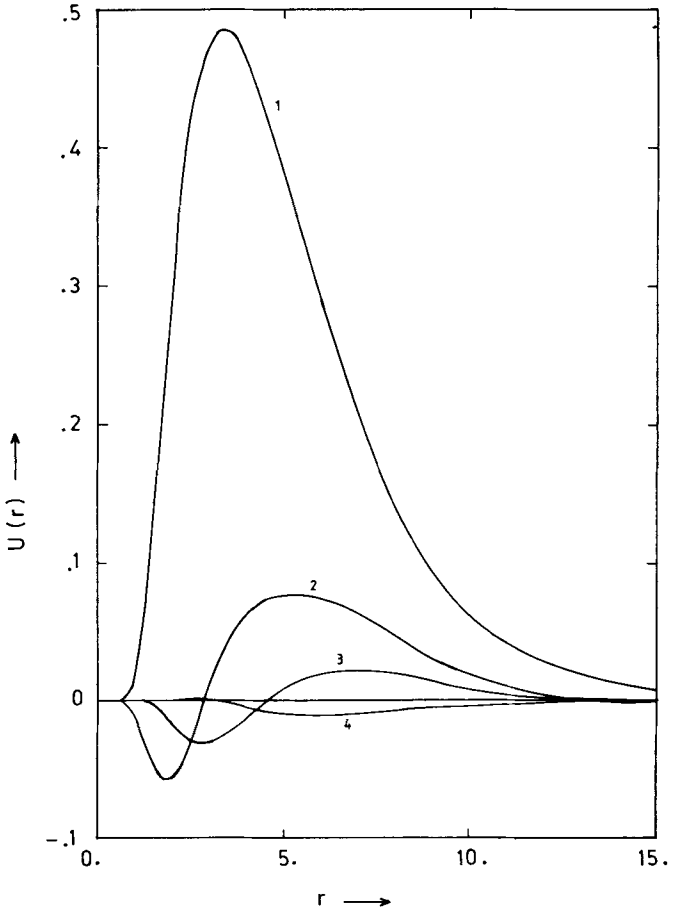

Figure 2. S state partial waves $U(r)$ for $K = 0$, 2, 4 and 10 (curve marked 1, 2, 3 and 4 respectively).

lower bounds of the exact binding energy [26], the latter being close to the UAA value. In table 6, we quote the results of careful Faddeev calculations [13] up to 34 channels. The UAA binding energy attained in the present calculation compares favourably with the 34 channel Faddeev result. From table 6, it is seen that P_D increases with increase in the number of channels, a trend similar to the HHE calculation with increasing partial waves, although the HHE value is larger than the Faddeev result.

4. Conclusion

In the first calculation of triton ground state with RSC potential by HHE method, the results obtained for the binding energy and the S, S' and D state probabilities compare favourably with those calculated by 34 channel Faddeev calculation. The D state probability calculated by HHE method is somewhat larger than that calculated by Faddeev method. The exact BE, which is larger than the UAA value, is also likely to

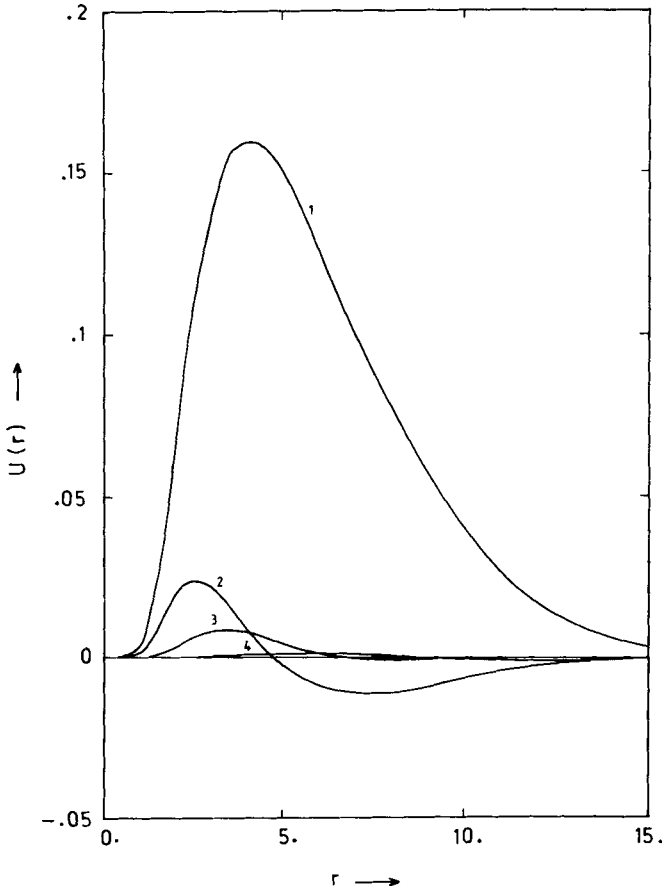

Figure 3. D state partial waves $U(r)$ for $K = 0$, 2, 4 and 10 (curve marked 1, 2, 3 and 4 respectively).

Table 5a. Value of C (in eq. (20)) from the least square fit.

K	EAA $-E(K)$	$-\Delta E_K$	$C \times 10^{-3}$	UAA $-E(K)$	$-\Delta E_K$	$C \times 10^{-3}$
6	4·67		24·362	3·786		24·291
		2·215			2·028	
9	6·885		24·036	5·814		24·201
		0·782			0·737	
12	7·667		24·419	6·551		24·305
		0·351			0·331	
15	8·018		24·272	6·882		24·266

be larger than 7·346 MeV obtained by 34 channel Faddeev calculation. These are probably related, since a higher D state probability produces larger S–D coupling and enhances the binding energy. However a conclusive remark can be made only after exact HHE calculation (without resorting to adiabatic approximations) is performed.

Table 5b. Extrapolated energy in MeV using relations (20) and (21).

K	EAA $-E(K)$	$-\Delta E_K$	UAA $-E(K)$	$-\Delta E_K$
18	8·195		7·051	
		0·099		0·095
21	8·294		7·146	
		0·060		0·058
24	8·354		7·204	
		0·038		0·037
27	8·392		7·241	
		0·026		0·025
30	8·418		7·266	
		0·017		0·017
33	8·435		7·283	
		0·013		0·012
36	8·448		7·295	
		0·009		0·009
39	8·457		7·304	
		0·007		0·007
42	8·464		7·311	
		0·005		0·005
45	8·469		7·316	

Table 6. Results of trinucleon Faddeev calculation for RSC potential.

Channel	BE	P_S	$P_{S'}$	P_D
3	6·384	90·08	1·91	8·01
5	7·023	88·91	1·67	9·34
9	7·210	88·88	1·60	9·43
18	7·231	89·04	1·46	9·42
26	7·342	89·01	1·41	9·50
34	7·346	89·02	1·40	9·50

Thus the present work fills in the gap left so far and provides the much needed check of the HHE method for a complete reliable calculation of the trinucleon system. Although the actual numerical calculations become prohibitively large for the inclusion of a large number of partial waves, the convergence theorems for hyperspherical harmonics expansion appear to be well obeyed and hence convergent binding energy can be extracted from the results with a finite number of partial waves. Although the number of channels in the Faddeev method is not directly related to the number of partial waves in the HHE method, the general convergence trends appear to be similar. The HHE provides more direct, physical insight since physical wave functions

are obtained simultaneously.

Acknowledgements

The work has been financed by the University Grants Commission, India through a Departmental Special Assistance grant to the Physics Department of the University of Calcutta. One of us (SB) acknowledges receipt of a senior research fellowship from the University of Burdwan, India.

Appendix A

1. *Coupling matrix for (SS) block*

$$\begin{aligned}\langle S,K|\,V(r_{12})|S,K'\rangle = {}^{(0)}N_{2K}\,{}^{(0)}N_{2K'}[{}^{(0)}F^{0,0}_{2K}\,{}^{(0)}F^{0,0}_{2K'}\times\\ \langle{}^{(2)}P^{0,0}_{2K}|0{\cdot}5\{V(^1S_0)+V_c(^3S_1-{}^3D_1)\}|{}^{(2)}P^{0,0}_{2K'}\rangle\\ +{}^{(0)}F^{2,2}_{2K}\,{}^{(0)}F^{2,2}_{2K'}\langle{}^{(2)}P^{2,2}_{2K}|0{\cdot}5(V_c(^3S_1-{}^3D_1)-3V_{LS}(^3S_1-{}^3D_1))\\ +2{\cdot}5V(^1D_2)+(5/6)\,V(^3D_2)|{}^{(2)}P^{2,2}_{2K'}\rangle]\end{aligned}\tag{A1}$$

2. *Coupling matrix for (S′S) block*

$$\begin{aligned}\langle S',K|\,V(r_{12})|S,K'\rangle = {}^{(+)}N_{2K}\,{}^{(0)}N_{2K'}[{}^{(+)}F^{0,0}_{2K}\,{}^{(0)}F^{0,0}_{2K'}\times\\ \langle{}^{(2)}P^{0,0}_{2K}|(1/2\sqrt{2})(V(^1S_0)-V_c(^3S_1-{}^3D_1))|{}^{(2)}P^{0,0}_{2K'}\rangle\\ +{}^{(+)}F^{2,2}_{2K}\,{}^{(0)}F^{2,2}_{2K'}\langle{}^{(2)}P^{2,2}_{2K}|(1/2\sqrt{2})\{(3V_{LS}(^3S_1-{}^3D_1)-V_c(^3S_1-{}^3D_1))\\ +5V(^1D_2)-5/3\,V(^3D_2)\}|{}^{(2)}P^{2,2}_{2K'}\rangle]\end{aligned}\tag{A2}$$

3. *Coupling matrix for (S′S′) block*

$$\begin{aligned}\langle S',K|\,V(r_{12})|S',K'\rangle = {}^{(+)}N_{2K}\,{}^{(+)}N_{2K'}[{}^{(+)}F^{0,0}_{2K}\,{}^{(+)}F^{0,0}_{2K'}\times\\ \langle{}^{(2)}P^{0,0}_{2K}|(1/4)(V(^1S_0)+V_c(^3S_1-{}^3D_1))|{}^{(2)}P^{0,0}_{2K'}\rangle\\ +{}^{(+)}F^{2,2}_{2K}\,{}^{(+)}F^{2,2}_{2K'}\langle{}^{(2)}P^{2,2}_{2K}|(1/4)\{(V_c(^3S_1-{}^3D_1)-3V_{LS}(^3S_1-{}^3D_1))\\ +5V(^1D_2)+5/3V(^3D_2)\}|{}^{(2)}P^{2,2}_{2K'}\rangle]\\ +{}^{(-)}N_{2K}\,{}^{(-)}N_{2K'}[{}^{(-)}F^{1,1}_{2K}\,{}^{(-)}F^{1,1}_{2K'}\times\langle{}^{(2)}P^{1,1}_{2K}|(1/12)\{(V(^3P_0)+3V(^3P_1)\\ +9V(^1P_1)+5(V_c(^3P_2-{}^3F_2)+V_{LS}(^3P_2-{}^3F_2))\}|{}^{(2)}P^{1,1}_{2K'}\rangle\\ +{}^{(-)}F^{3,3}_{2K}\,{}^{(-)}F^{3,3}_{2K'}\langle{}^{(2)}P^{3,3}_{2K}|(1/12)5(V_c(^3P_2-{}^3F_2)\\ -4V_{LS}(^3P_2-{}^3F_2))|{}^{(2)}P^{3,3}_{2K'}\rangle]\end{aligned}\tag{A3}$$

4. *Coupling matrix for (D,S)* block

$$\begin{aligned}\langle D^+,K|\,V(r_{12})|S,K'\rangle = {}^{(D+)}N_{2K+2}\,{}^{(0)}N_{2K'}[{}^{(D+)}F^{2,2}_{2K+2}\,{}^{(0)}F^{2,2}_{2K'}\times\\ \langle{}^{(2)}P^{2,2}_{2K+2}|(-1/\sqrt{2})\,V_T(^3S_1-{}^3D_1)|{}^{(2)}P^{2,2}_{2K'}\rangle\\ -{}^{(D+)}F^{0,2}_{2K+2}\,{}^{(0)}F^{0,0}_{2K'}\langle{}^{(2)}P^{0,2}_{2K+2}|\sqrt{2}V_T(^3S_1-{}^3D_1)|{}^{(2)}P^{0,0}_{2K'}\rangle\\ -{}^{(D+)}F^{2,0}_{2K+2}\,{}^{(0)}F^{2,2}_{2K'}\langle{}^{(2)}P^{2,0}_{2K+2}|\sqrt{2}V_T(^3S_1-{}^3D_1)|{}^{(2)}P^{2,2}_{2K'}\rangle]\end{aligned}\tag{A4}$$

5. *Coupling matrix for (D, S′) block*

$$\begin{aligned}
\langle D,K|V(r_{12})|S',K'\rangle &= {}^{(D+)}N_{2K+2}\,{}^{(+)}N_{2K'}[{}^{(D+)}F^{2,2}_{2K+2}\,{}^{(+)}F^{2,2}_{2K'}\times\\
&\langle{}^{(2)}P^{2,2}_{2K+2}|0{\cdot}5V_T({}^3S_1-{}^3D_1)|{}^{(2)}P^{2,2}_{2K'}\rangle\\
&+{}^{(D+)}F^{0,2}_{2K+2}\,{}^{(+)}F^{0,0}_{2K'}\langle{}^{(2)}P^{0,2}_{2K+2}|\,V_T({}^3S_1-{}^3D_1)|{}^{(2)}P^{0,0}_{2K'}\rangle\\
&+{}^{(D+)}F^{2,0}_{2K+2}\,{}^{(+)}F^{2,2}_{2K'}\langle{}^{(2)}P^{2,0}_{2K+2}|\,V_T({}^3S_1-{}^3D_1)|{}^{(2)}P^{2,2}_{2K'}\rangle]\\
&+{}^{(D-)}N_{2K+2}\,{}^{(-)}N_{2K'}[{}^{(D-)}F^{1,1}_{2K+2}\,{}^{(-)}F^{1,1}_{2K'}\times\\
&\langle{}^{(2)}P^{1,1}_{2K+2}|(-1/30)\,V_T({}^3P_2-{}^3F_2)|{}^{(2)}P^{1,1}_{2K'}\rangle\\
&-{}^{(D-)}F^{3,1}_{2K+2}\,{}^{(-)}F^{3,3}_{2K'}\langle{}^{(2)}P^{3,1}_{2K+2}|(9/5)\,V_T({}^3P_2-{}^3F_2)|{}^{(2)}P^{3,3}_{2K'}\rangle\\
&-{}^{(D-)}F^{1,3}_{2K+2}\,{}^{(-)}F^{1,1}_{2K'}\langle{}^{(2)}P^{1,3}_{2K+2}|(9/5)\,V_T({}^3P_2-{}^3F_2)|{}^{(2)}P^{1,1}_{2K'}\rangle\\
&-{}^{(D-)}F^{3,3}_{2K+2}\,{}^{(-)}F^{3,3}_{2K'}\langle{}^{(2)}P^{3,3}_{2K+2}|(8/15)\,V_T({}^3P_2-{}^3F_2)|{}^{(2)}P^{3,3}_{2K'}\rangle]
\end{aligned}\tag{A5}$$

6. *Coupling matrix for (D, D) block*

$$\begin{aligned}
\langle D,K|V(r_{12})|D,K'\rangle &= {}^{(D+)}N_{2K+2}\,{}^{(D+)}N_{2K'+2}[{}^{(D+)}F^{2,2}_{2K+2}\,{}^{(D+)}F^{2,2}_{2K'+2}\times\\
&\langle{}^{(2)}P^{2,2}_{2K+2}|(1/4)\{(V_c({}^3S_1-{}^3D_1)-3V_{LS}({}^3S_1-{}^3D_1))\\
&-2V_T({}^3S_1-{}^3D_1)+5/3V({}^3D_2)\}|{}^{(2)}P^{2,2}_{2K'+2}\rangle\\
&+{}^{(D+)}F^{2,0}_{2K+2}\,{}^{(D+)}F^{2,0}_{2K'+2}\langle{}^{(2)}P^{2,0}_{2K+2}|0{\cdot}5V_c({}^3S_1-{}^3D_1)|{}^{(2)}P^{2,0}_{2K'+2}\rangle\\
&-{}^{(D+)}F^{2,0}_{2K+2}\,{}^{(D+)}F^{2,2}_{2K'+2}\langle{}^{(2)}P^{2,0}_{2K+2}|\,V_T({}^3S_1-{}^3D_1)|{}^{(2)}P^{2,2}_{2K'+2}\rangle\\
&-{}^{(D+)}F^{2,2}_{2K+2}\,{}^{(D+)}F^{2,0}_{2K'+2}\langle{}^{(2)}P^{2,2}_{2K+2}|\,V_T({}^3S_1-{}^3D_1)|{}^{(2)}P^{2,0}_{2K'+2}\rangle\\
&+{}^{(D+)}F^{0,2}_{2K+2}\,{}^{(D+)}F^{0,2}_{2K'+2}\langle{}^{(2)}P^{0,2}_{2K+2}|(1/2)\times\\
&\{V_c({}^3S_1-{}^3D_1)-3V_{LS}({}^3S_1-{}^3D_1)-2V_T({}^3S_1-{}^3D_1)\}|{}^{(2)}P^{0,2}_{2K'+2}\rangle]\\
&+{}^{(D-)}N_{2K+2}\,{}^{(D-)}N_{2K'}[{}^{(D-)}F^{1,1}_{2K+2}\,{}^{(D-)}F^{1,1}_{2K'}\times\\
&\langle{}^{(2)}P^{1,1}_{2K+2}|\{1/3V({}^3P_0)+1/4V({}^3P_1)-1/150V_T({}^3P_2-{}^3F_2)\\
&+1/60(V_c({}^3P_2-{}^3F_2)+V_{LS}({}^3P_2-{}^3F_2)\}|{}^{(2)}P^{1,1}_{2K'+2}\rangle\\
&+{}^{(D-)}F^{3,1}_{K+2}\,{}^{(D-)}F^{3,1}_{2K'}\langle{}^{(2)}P^{3,1}_{2K+2}|\{-9/25V_T({}^3P_2-{}^3F_2)\\
&+0{\cdot}9(V_c({}^3P_2-{}^3F_2)+V_{LS}({}^3P_2-{}^3F_2))\}|{}^{(2)}P^{3,1}_{2K'+2}\rangle\\
&+{}^{(D-)}F^{1,3}_{K+2}\,{}^{(D-)}F^{1,3}_{2K'+2}\langle{}^{(2)}P^{1,3}_{2K+2}|\{-1{\cdot}44V_T({}^3P_2-{}^3F_2)\\
&+0{\cdot}9(V_c({}^3P_2-{}^3F_2)-4V_{LS}({}^3P_2-{}^3F_2))\}|{}^{(2)}P^{1,3}_{2K'+2}\rangle\\
&-{}^{(D-)}F^{1,1}_{K+2}\,{}^{(D-)}F^{1,3}_{2K'+2}\langle{}^{(2)}P^{1,1}_{2K+2}|9/25V_T({}^3P_2-{}^3F_2)|{}^{(2)}P^{1,3}_{2K'+2}\rangle\\
&-{}^{(D-)}F^{3,1}_{K+2}\,{}^{(D-)}F^{3,3}_{2K'+2}\langle{}^{(2)}P^{3,1}_{2K+2}|1{\cdot}44V_T({}^3P_2-{}^3F_2)|{}^{(2)}P^{3,3}_{2K'+2}\rangle\\
&-{}^{(D-)}F^{1,3}_{K+2}\,{}^{(D-)}F^{1,1}_{2K'+2}\langle{}^{(2)}P^{1,3}_{2K+2}|9/25V_T({}^3P_2-{}^3F_2)|{}^{(2)}P^{1,1}_{2K'+2}\rangle\\
&-{}^{(D-)}F^{3,3}_{K+2}\,{}^{(D-)}F^{3,1}_{2K'+2}\langle{}^{(2)}P^{3,3}_{2K+2}|1{\cdot}44V_T({}^3P_2-{}^3F_2)|{}^{(2)}P^{3,1}_{2K'+2}\rangle\\
&+{}^{(D-)}F^{3,3}_{K+2}\,{}^{(D-)}F^{3,3}_{2K'+2}\langle{}^{(2)}P^{3,3}_{2K+2}|(-32/75)\,V_T({}^3P_2-{}^3F_2)\\
&+4/15(V_c({}^3P_2-{}^3F_2)-4V_{LS}({}^3P_2-{}^3F_2))|{}^{(2)}P^{3,3}_{2K'+2}\rangle]
\end{aligned}\tag{A6}$$

The numerical factors arise from angular momentum coupling coefficients.

Appendix B

The various components of the RSC potential in MEV (corresponding to isospin $(t) = 1$) are given in eqs (B.1) through (B.5), where $h = 10{\cdot}463$ MeV and $x = \mu r$ with $\mu = 0{\cdot}7F^{-1}$ and r is the distance between the interacting two nucleons.

1. *Singlet even components*

$$V(^1S_0) = -h\frac{\exp(-x)}{x} - 1650{\cdot}6\frac{\exp(-4x)}{x} + 6484{\cdot}2\frac{\exp(-7x)}{x} \tag{B1}$$

$$V(^1D_2) = -h\frac{\exp(-x)}{x} - 12{\cdot}322\frac{\exp(-2x)}{x} - 1112{\cdot}6\frac{\exp(-4x)}{x} + 6484{\cdot}2\frac{\exp(-7x)}{x} \tag{B2}$$

2. *Triplet odd components*

$$V(^3P_0) = -h\left[\left(1+\frac{4}{x}+\frac{4}{x^2}\right)\exp(-x) - \left(\frac{16}{x}+\frac{4}{x^2}\right)\exp(-4x)\right]\Big/x + 27{\cdot}133\frac{\exp(-2x)}{x} - 790{\cdot}74\frac{\exp(-4x)}{x} + 20662\frac{\exp(-7x)}{x} \tag{B3}$$

$$V(^3P_1) = h\left[\left(1+\frac{2}{x}+\frac{2}{x^2}\right)\exp(-x) - \left(\frac{8}{x}+\frac{2}{x^2}\right)\exp(-4x)\right]\Big/x - 135{\cdot}25\frac{\exp(-2x)}{x} + 472{\cdot}81\frac{\exp(-3x)}{x} \tag{B4}$$

$$V(^3P_2 - {}^3F_2) = V_C + V_T S_{12} + V_{LS}\mathbf{L}\cdot\mathbf{S} \tag{B5}$$

where,

$$V_C = \frac{h}{3}\frac{\exp(-x)}{x} - 933{\cdot}48\frac{\exp(-4x)}{x} + 4152{\cdot}1\frac{\exp(-6x)}{x}$$

$$V_T = h\left[\left(1/3+\frac{1}{x}+\frac{1}{x^2}\right)\exp(-x) - \left(\frac{4}{x}+\frac{1}{x^2}\right)\exp(-4x)\right]\Big/x - 34{\cdot}925\frac{\exp(-3x)}{x}$$

$$V_{LS} = -2074{\cdot}1\frac{\exp(-6x)}{x}.$$

The components of the RSC potentials in MeV corresponding to isospin zero are presented in eq. B6 through B8.

3. *Singlet odd components*

$$V(^1P_1) = 3h\frac{\exp(-x)}{x} - 634{\cdot}39\frac{\exp(-2x)}{x} + 2163{\cdot}4\frac{\exp(-3x)}{x} \tag{B6}$$

4. *Triplet even components*

$$V(^3D_2) = -3h\left[\left(1+\frac{2}{x}+\frac{2}{x^2}\right)\exp(-x) - \left(\frac{8}{x}+\frac{2}{x^2}\right)\exp(-4x)\right]\Big/x$$
$$- 220{\cdot}12\frac{\exp(-2x)}{x} + 871{\cdot}0\frac{\exp(-3x)}{x} \tag{B7}$$

$$V(^3S_1 - {}^3D_1) = V_C + V_T S_{12} + V_{LS}\mathbf{L}\cdot\mathbf{S} \tag{B8}$$

where

$$V_C = -h\frac{\exp(-x)}{x} + 105{\cdot}468\frac{\exp(-2x)}{x} - 3187{\cdot}8\frac{\exp(-4x)}{x}$$
$$+ 9924{\cdot}3\frac{\exp(-6x)}{x}$$

$$V_T = -h\left[\left(1+\frac{3}{x}+\frac{3}{x^2}\right)\exp(-x) - \left(\frac{12}{x}+\frac{3}{x^2}\right)\exp(-4x)\right]\Big/x$$
$$+ 351{\cdot}77\frac{\exp(-4x)}{x} - 1673{\cdot}5\frac{\exp(-6x)}{x}$$

$$V_{LS} = 708{\cdot}91\frac{\exp(-4x)}{x} - 2713{\cdot}1\frac{\exp(-6x)}{x}$$

V_C, V_{LS} and V_T represent central, spin-orbit and tensor term of the RSC potential respectively. S_{12} is the usual tensor operator.

References

[1] Y A Simonov, in *Proceedings of the International Symposium on the Present Status and Novel Developments in the Nuclear Many body Problems*, Rome, 1972, edited by F Calogera and C Ciofi degli Atti (Editrice Compsitori, Bologna, 1974), p. 527

[2] J Bruinsma, R V Wageningen and J L Visschers, in *Few particle problems in Nuclear interaction* edited by I Slaus (North-Holland, Amsterdam, 1973) p. 368

[3] V F Demin and Y E Pokrovsky, *Phys. Lett.* **B47**, 394 (1973)

[4] G Erens, J L Visschers and R V Wageningen, *Ann. Phys.* **67**, 461 (1971)

[5] J L Ballot and M Fabre de la Ripelle, *Ann. Phys. (N.Y.)* **127**, 62 (1980)

[6] T K Das, H T Coelho and M Fabre de la Ripelle, *Phys. Rev.* **C26**, 2288 (1982)
T K Das and H T Coelho, *Phys. Rev.* **C26**, 697 (1982)
T B De and T K Das, *Phys. Rev.* **C36**, 402 (1987)

[7] A K Ghosh and T K Das, *Phys. Rev.* **C42**, 1249 (1990)

[8] V B Mandelzweig, *Nucl. Phys.* **A508** 63c (1990)

[9] L D Faddeev, *Zh. Eksp. Teor. Fiz.* **39**, 1459 (1960)
L D Faddeev, *Sov. Phys. JETP* **12**, 1014 (1961)

[10] R Reid, *Ann. Phys. (NY)* **50**, 411 (1968)

[11] G L Payne, J L Friar, B F Gibson and I R Afnan, *Phys. Rev.* **C22**, 823 (1980)
C Hajduk and P U Sauer, *Nucl. Phys.* **A369**, 321 (1981)
J L Friar, B F Gibson and G L Payne, *Phys. Rev.* **C37**, 2869 (1988)

[12] T Sasakawa and T Sawada, *Phys. Rev.* **C20**, 1954 (1979)
G L Payne, J L Friar and B F Gibson, *Phys. Rev.* **C22**, 832 (1980)
T Sasakawa, H Okuno and T Sawada, *Phys. Rev.* **C23**, 905 (1981)
S Ishikawa, T Sasakawa, T Sawada and T Ueda, *Phys. Rev. Lett.* **53**, 1877 (1984)
[13] C R Chen, G L Payne, J L Friar and B F Gibson, *Phys. Rev.* **C31**, 2266 (1985)
[14] M I Mukhtarova, *Sov. J. Nucl. Phys.* **49** 208 (1989)
[15] D Gogny, P Pires and R de Tourreil, *Phys. Lett.* **B32**, 591 (1970)
[16] R de Tourreil and D W I Sprung, *Nucl. Phys.* **A201**, 193 (1973)
[17] R de Tourreil, B Rouben and D W I Sprung, *Nucl. Phys.* **A242**, 445 (1975)
J Côte, *et al Nucl. Phys.* **A273**, 269 (1976)
[18] T R Schneider, *Phys. Lett.* **B40**, 439 (1972)
[19] T K Das and S Bhattacharyya, *Pramana – J. Phys.* **40**, 189 (1993)
[20] M K Pal, *Theory of Nuclear Structure*, Affliated East-West Press Pvt Ltd, New Delhi (1982) p. 30
[21] T K Das and T B De, *Pramana – J. Phys.* **28**, 645 (1987)
T B De and T K Das, *Phys. Rev.* **C36**, 402 (1987)
[22] S Bhattacharyya and T K Das, *J. Comput. Phys.* (*NY*) **114**, 308 (1994)
[23] B R Johnson, *J. Chem. Phys.* **69**, 4678 (1978)
[24] T K Das, H T Coelho and M Fabre de la Ripelle, *Phys. Rev.* **C26**, 2281 (1982)
[25] J L Ballot, M Beiner and M Fabre de la Ripelle, in *Present status and novel developments in the nuclear many body problems*, edited by F Calogera and C Ciofi degli Atti, (Rome 1972) p. 565
[26] J L Ballot, M Fabre de la Ripelle and J S Levinger, *Phys. Rev.* **C26**, 2301 (1982)